J. Math. Biol. (2006) 53:585–616
DOI 10.1007/s00285-006-0017-y

Mathematical Biology

M^5 mesoscopic and macroscopic models for mesenchymal motion

Thomas Hillen

Received: 21 September 2005 / Revised: 20 April 2006 /
Published online: 5 July 2006

Abstract In this paper mesoscopic (individual based) and macroscopic (population based) models for mesenchymal motion of cells in fibre networks are developed. Mesenchymal motion is a form of cellular movement that occurs in three-dimensions through tissues formed from fibre networks, for example the invasion of tumor metastases through collagen networks. The movement of cells is guided by the directionality of the network and in addition, the network is degraded by proteases. The main results of this paper are derivations of mesoscopic and macroscopic models for mesenchymal motion in a timely varying network tissue. The mesoscopic model is based on a transport equation for correlated random walk and the macroscopic model has the form of a drift-diffusion equation where the mean drift velocity is given by the mean orientation of the tissue and the diffusion tensor is given by the variance-covariance matrix of the tissue orientations. The transport equation as well as the drift-diffusion limit are coupled to a differential equation that describes the tissue changes explicitly, where we distinguish the cases of directed and undirected tissues. As a result the drift velocity and the diffusion tensor are timely varying. We discuss relations to existing models and possible applications.

1 Introduction

In a review article on cell movement, Friedl and Bröcker [10] report that the movement of amoeboid cells on a surface differs significantly from their

Dedicated to K.P. Hadeler, a great scientist, teacher, and friend.

T. Hillen (✉)
University of Alberta, Edmonton, AB, Canada T6G2G1
e-mail: thillen@ualberta.ca

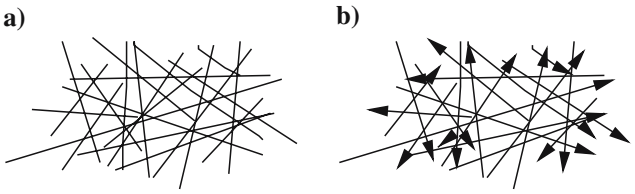

Fig. 1 A sketch of an undirected tissue in (**a**) and a directed tissue in (**b**)

movement in a tissue matrix. On flat surfaces (like a petri dish) cells are free to move in any direction, and they can form multiple adhesions with the substrate. In many cases cells appear round-shaped with broad protrusions in the direction of movement. In three dimensional tissues, however, cells experience movement constraints given from the surrounding tissue. Some tumor cells, for example, appear elongated and spindle shaped. They send out thin pseudopods for directional guidance from the surrounding matrix. Moreover, the cells use proteases to alter the tissue and to cut through obstacles. This form of motion is termed *mesenchymal* motion [10,11].

In this paper we derive and analyze transport models for mesenchymal motion and we study the corresponding drift-diffusion limits. Transport models are also seen as *mesoscopic* models which simplify the microscopic details, but still allow for an individual-based model. Scaling arguments are used to derive corresponding macroscopic models which describe a population of cells as a whole. These models typically take the form of drift-diffusion equations. Macroscopic models are very useful to describe the dynamic behavior of moving cells in tissues and they can be easily extended to include interactions with the immune system, the invasion of harmful metastases, or guided movement due to chemotaxis.

The main result of this paper are the derivation of kinetic models for mesenchymal cell movement in network tissues, their drift-diffusion scaling limits, and a discussion of the corresponding one-dimensional versions. The whole analysis is divided into undirected and directed tissue (explained below). The transport models are given in (12) for undirected tissue and in (17) for directed tissue. The corresponding one-dimensional versions are given in (27) for undirected tissue and in (20) for directed tissue. The macroscopic drift-diffusion limits are given in (60)–(64) for undirected tissue and in (67)–(70) for directed tissue.

In *undirected tissues* the fibres are symmetrical along their axis and both fibre directions are identical (see Fig. 1a)). Collagen fibres are undirected and they form the basis for many human (and animal) tissues. It is of utmost importance to understand the movement behavior of cells in tissues and to attempt to model the cell–tissue interactions. The tissue morphology can be of very different nature: from the elongated and parallel-oriented fibres of type I collagen, to the network-like fibres of type IV collagen. An overview of relevant tissue matrices can be found in Yurchenko et al. [25].

For *directed tissues* (Fig. 1b) the fibres are unsymmetrical and the two ends can be distinguished (positive/negative, forward/backward, north/south). Directed components do not play a major role for cell movement in tissues, however, directed fibres occur inside cells (such as tubulin or actin) or as combination of cells (such as the fibre tracks in the white matter of the brain). Branching collagen fibre networks can also be considered directional if the branching points are of significance for the movement of cells. As mentioned already, the undirected case is more important for the application in mind. From the mathematical point of view, the directed case is also of interest and in this paper we treat both cases. It is beneficial to have a general theory, since in the future directed fibres might be identified in the extracellular matrix (ECM) that play an important role for cell movement.

According to Friedl and Bröcker [10], the movement of mesenchymal cells in tissues can be split into three processes (1) attachment of the leading edge, (2) cell contraction and (3) detachment of the cell rear [10]. The attachment is typically integrin-mediated and some cells form focal adhesion points with the tissue fibres. The focal adhesion points connect the integrin binding site to the cytoskeleton of the cell. The integrin-mediated binding leads to the spindle-like morphology of the cells. In experiments with HT-1080 fibrosarcoma cells and with MDA-MB-231 mammarian carcinoma cells it has been observed by Wolf et al. [24] that ECM-degrading proteases are expressed to degrade the collagen tissue and to form tube-like matrix defects. When the ECM-degrading enzyme is inhibited and the integrins are blocked, then the cells are no longer spindle shaped and they will no longer form tunnel-shaped tracks. However, they are still able to translocate and in some cases they have been found to form constriction rings to squeeze through obstacles [24]. This effect has been called mesenchymal–amoeboid transition [11].

The models derived here are based on directional information about the underlying tissue network. This complements recent development in MRI spectroscopy, where tissue directionality and tissue fibres can be visualized. The method is called *diffusion tensor imaging* (DTI) [3] and MRI spectroscopy is used to measure the diffusion of water molecules in the tissue for several directions. The method has been used by Mori et al. [17] to identify white matter fibre tracks in the rat brain. So far the resolution of DTI scanning is about 2 mm for six possible directions [3], it can be expected that further development of this technique will improve the resolution. If DTI measurements become available I plan to use the models of this paper to study cell movement in these tissues. This could be of importance to glioma invasion within the brain.

Models for orientational movement were also studied by Alt [1], Dickinson [7], Othmer et al. [18], Hillen and Othmer [14], [19], or more recent publications by Chalub et al. [4] and Hwang et al. [15]. For time-stationary tissues the model presented here falls into the general class of transport equations for *contact guidance*, that have been introduced and studied by Dickinson [7]. However, as Dickinson uses projection operators, I use hydrodynamic scaling and the Chapman–Enskog expansion. The drift-diffusion limit of those two methods is

the same (see Sect. 6 for a more detailed comparison). Dickinson extends his theory in [7] to time-varying tissue where the variations in tissue occur on a slower timescale than particle movement. With the method proposed here the time scales of movement and tissue changes do not need to be separated and a dynamic drift-diffusion limit is derived, where the parameters (diffusion tensor, and drift velocity) dynamically depend on the changing environment.

Barocas and Tranquillo [2] developed the *anisotropic biphasic theory* (ABT) for contact guidance. The ABT is based on balance equations between the tissue–cell phase and the interstitial fluid phase, where cell alignment and fibre alignment are included. We give a more detailed comparison in the discussion Sect. 6.

Dallon et al. [5], [6] derived and studied a mathematical model for collagen fibre deposition by moving fibroblasts and application to wound healing. Their model uses integration kernels that describe the interaction between cell fibres. These terms lead to orientational diffusion terms in the corresponding mathematical model. Orientational diffusion is neglected here, since we assume strong contact guidance by the fibre network (as dominating effect).

The paper is organized as follows: In Sect. 2 a transport model for movement in a timely varying tissue matrix is introduced and a dynamic equation for the tissue changes is derived. We distinguish between directed and undirected tissue and derive for each case a coupled system of a transport equation for the cells and a differential equation for the directional distribution of the fibre network. The mesoscopic models for mesenchymal motion are given in (12) for undirected tissue and in (17) for directed tissue.

In Sect. 3 the analysis of the one-dimensional versions is given. Here the important steps are easily done explicitly and some basic insight can be gained already. Three scaling arguments are introduced and it is shown how they are related. These are (1) the moment closure, (2) the parabolic scaling, and (3) the hydrodynamic scaling.

In Sect. 4 the n-dimensional transport model for mesenchymal motion in a given tissue matrix is studied. Again (1) the moment closure method, (2) the parabolic scaling and (3) the hydrodynamic scaling are investigated. The hydrodynamic scaling gives the fullest picture as it shows how drift dominates and diffusion appears as a correction term. The methods used in Sect. 4 closely follow the exposition of Dolak and Schmeiser [9] for chemotaxis models. The methods carry over, although the model studied here is not a special case of the model of Dolak and Schmeiser, so the results of [9] cannot be used here.

In Sect. 5 the hydrodynamic scaling is carried out for the full models of mesenchymal motion in a tissue which is cut by protease released by the cells. Here the macroscopic limit models are derived, Eqs. (60)–(64) for the undirected case and Eqs. (67)–(70) for the directed case. The general derivations are applied to the one-dimensional cases and the results are compared to those from Sect. 3.

In Sect. 6 the conclusions are summarized and compared to existing theories from the literature. Moreover, future venues for analysis, numerical simulation, extensions, and applications are discussed.

2 Transport model for mesenchymal motion

To model the movement of a cell in a given fibre network we assume that the matrix or tissue gives a selection of preferred directions along which a cell can move. Let S^{n-1} denote the unit sphere in $\mathbb{R}^n$ and let $\theta \in S^{n-1}$ denote the fibre orientation. Then we denote the distribution of fibre orientations at time $t \geq 0$ and at location $x \in \Omega$ by the probability density $q(t,x,\theta)$. The n-dimensional spatial domain Ω is not specified further. Of course we assume for all t,x that

$$\int_{S^{n-1}} q(t,x,\theta)\mathrm{d}\theta = 1.$$

We define the first two-directional moments of q and introduce the vector of the *mean fibre direction* as

$$\mathbb{E}_q(t,x) := \int_{S^{n-1}} \theta q(t,x,\theta)\mathrm{d}\theta \tag{1}$$

and the *variance-covariance matrix* of q as

$$\mathbb{V}_q(t,x) := \int_{S^{n-1}} (\theta - \mathbb{E}_q)(\theta - \mathbb{E}_q)^T q(t,x,\theta)\mathrm{d}\theta. \tag{2}$$

For undirected fibres we add the requirement of symmetry, such that

$$q(t,x,\theta) = q(t,x,-\theta) \quad \text{for undirected tissues.}$$

This has the immediate consequence that

$$\mathbb{E}_q(t,x) = 0 \quad \text{and} \quad \mathbb{V}_q(t,x) = \int_{S^{n-1}} \theta\theta^T q(t,x,\theta)\mathrm{d}\theta \quad \text{for undirected tissues.} \tag{3}$$

2.1 Cell movement

Since the fibre network gives directional information about possible movement directions of the cells, a transport equation approach seems natural. In this approach we assume that cell–cell interactions play a negligible role. The primary interaction studied here are cell–fibre interaction. To properly include cell–cell interactions a stochastic many particle system needs to be studied; this has been done for chemotaxis in [21].

Let V denote the set of all possible velocities of moving cells and $p(t,x,v)$ the population density of cells that have velocity vector v at time t at location x. For our purpose $p(t,x,v)$ can also be interpreted as probability density to find a

moving cell at time t at location x with velocity v. We assume that V is radially symmetric and can be written as

$$V = [s_1, s_2] \times S^{n-1}, \quad 0 \le s_1 \le s_2 < \infty,$$

where $[s_1, s_2]$ is the range of possible speeds. For now we assume that there is a constant turning rate μ. We assume that if cells decide to change direction, they will choose a new direction $\theta \in S^{n-1}$ with probability $q(t,x,\theta)$. Where we assume that if a direction θ is chosen, then the speed s will be chosen randomly such that $s\theta \in V$. We introduce a notation for the unit vector in direction of v

$$\hat{v} := \frac{v}{\|v\|},$$

and we define a weight parameter:

$$\omega := \int_V q(t,x,\hat{v}) \mathrm{d}v = \begin{cases} \frac{s_2^n - s_1^n}{n} & \text{for } s_1 < s_2, \\ s^{n-1} & \text{for } s_1 = s_2 = s. \end{cases} \tag{4}$$

Then the transport model for mesenchymal motion in a timely varying directional field reads

$$p_t(t,x,v) + v \cdot \nabla p(t,x,v) = -\mu p(t,x,v) + \mu \int_V \frac{q(t,x,\hat{v})}{\omega} p(t,x,v') \mathrm{d}v'.$$

Note that since q is a probability distribution on S^{n-1} the quotient $q(t,x,\hat{v})/\omega$ is a distribution on V and

$$\int_V \frac{q(t,x,\hat{v})}{\omega} \mathrm{d}v = 1.$$

Hence our basic assumption can be formulated that $q(t,x,\hat{v})/\omega$ gives the distribution of newly chosen velocities. In a short notation the above transport equation reads:

$$p_t + v \cdot \nabla p = -\mu p + \mu \frac{q(t,x,\hat{v})}{\omega} \bar{p}, \quad \bar{p} = \int_W p(v) \mathrm{d}v. \tag{5}$$

In a next step we model the tissue changes explicitly.

2.2 Modeling tissue changes

To model tissue changes we are interested to derive an equation for $q(t,x,\theta)$ of the form

$$q_t(t,x,\theta) = G(\theta,p,q). \tag{6}$$

Since q describes a non negative probability distribution on the unit sphere S^{n-1}, we stipulate the following minimal assumptions on the fibre dynamics G:

$$\int_{S^{n-1}} G(\theta,.,.)\mathrm{d}\theta = 0, \quad G(.,.,0) = 0, \tag{7}$$

with an additional symmetry assumption for undirected tissue

$$G(-\theta,p,q) = G(\theta,p,q).$$

In general the function $G(\theta,p,q)$ can describe fibre degradation, fibre generation (through fibroblasts) or other fibre–cell interactions. Here we focus on proteolytic fibre degradation, and we derive two possible choices of G for mesenchymal motion.

In general, Eqs. (5) and (6) form a dynamical system for cell movement in a fibre network including fibre network dynamics; and we can ask the question of local and global existence of solutions. In case of chemotaxis, a system of a transport equation and a parabolic equation for the chemical signal was studied recently by Chalub et al. [4] and Hwang et al. [15]. Their proofs of global existence of solutions are based on L^∞ estimates of the turning kernel. In the case studied here the turning kernel is given by the distribution q. In examples, later, we like to be able to consider totally aligned tissues, which for a tissue in direction of $b \in \mathbb{R}^n$ corresponds to $q(\theta) = \delta_b(\theta)$. Hence a solution theory should include δ-distributions for q. Of course, these are not bounded in L^∞. In particular, assumption (A0) in [4] does not apply, and hence their results cannot be applied directly. At a first glance it seems that a detailed existence analysis of model (5) and (6) is technically involved. In this paper we rather focus on the modeling itself and we keep the existence questions in mind for future research.

To model the proteolytic interactions of the metastatic cells with the fibre network, we first introduce the fibre density $Q(t,x,\theta)$ and we distinguish the two tissue types.

We assume that, as cells move through the tissue by contact guidance, they primarily cut directions that are orthogonal to the direction of movement. This assumption is supported by the observation that the proteolytic activity in the cell front is enhanced compared to the sides or the rear of the cell (see Wolf et al. [24]). Further we assume that the cells leave fibres intact that are parallel to the movement direction.

2.2.1 Undirected tissue

We compare the fibre direction $\theta \in S^{n-1}$ with the movement direction $v \in V$ of a cell.

1. If the tissue fibre θ is orthogonal to $\hat{v}$ ($|\theta \cdot \hat{v}| \approx 0$), then the cell will cut this fibre with a high probability. On the other hand, if θ is oriented parallel to $\hat{v}$ ($|\theta \cdot \hat{v}| \approx 1$), then it is most likely not cut. We define the mean projection of movement direction on the fibre orientation:

$$\Pi_u(t,x,\theta) = \frac{1}{\bar{p}(t,x)} \int_V |\theta \cdot \hat{v}| p(t,x,v) \mathrm{d}v, \tag{8}$$

   which satisfies

$$0 \le \Pi_u \le 1.$$

   The case $\Pi_u(t,x,\theta) = 0$ corresponds to the case where all cells are moving perpendicular to θ and we expect fibre degradation. The case of $\Pi_u(t,x,\theta) = 1$ corresponds to total alignment in the directions $\pm\theta$.
2. Further we assume that the mass-action term $\bar{p}Q$ describes the frequency of an encounter of a tissue fibre with a cell.
3. Moreover, we introduce a constant $\kappa \ge 0$ that describes the efficiency of cutting or the concentration of the protease per cell.

Based on these assumptions, our tissue modification model for the fibre density $Q(t,x,\theta)$ has the form

$$Q_t(t,x,\theta) = \kappa(\Pi_u(t,x,\theta) - 1)\, \bar{p}\, Q. \tag{9}$$

The above transport model (5) uses the directional distribution $q(t,x,\theta)$. This is given, for $Q \neq 0$ by

$$q(t,x,\theta) = \frac{Q(t,x,\theta)}{\int_{S^{n-1}} Q(t,x,\theta)\mathrm{d}\theta}.$$

Then from (9) we derive a differential equation for q:

$$q_t(t,x,\theta) = \kappa(\Pi_u(t,x,\theta) - A_u(t,x))\, \bar{p}(t,x) q(t,x,\theta), \tag{10}$$

with

$$A_u(t,x) = \int_{S^{n-1}} \Pi_u(t,x,\theta) q(t,x,\theta) \mathrm{d}\theta. \tag{11}$$

It can be easily verified that $q(t,x,\theta)$ is indeed a probability density for $\theta \in S^{n-1}$, i.e. $q \ge 0$ and $\int q \mathrm{d}\theta = 1$. An interpretation of Eq. (10) is shown in Fig. 2. As

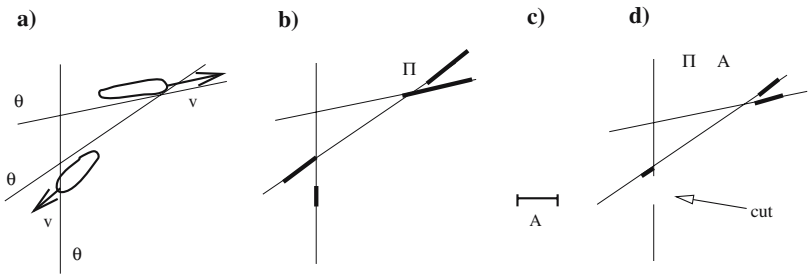

Fig. 2 (**a**) three fibres and two moving cells are sketched. (**b**) The projections Π_u of the cell movement directions onto the three fibres. The coefficient A_u calculates the mean length of these projections, as shown in (**c**). (**d**) The projection Π_u is compared to the mean length A_u and if this value is negative the fibre will be degraded

$\Pi_u(t,x,\theta)$ denotes the mean projection of cell movement directions $\hat{v}$ onto a given orientation θ, the term $A_u(t,x)$ denotes the mean value of these mean projections over all fibre directions. $A_u(t,x)$ is a measure of the relative alignment of fibres and cells. The differential equation (10) compares the projection of the fibre direction with its mean value. If $\Pi_u(t,x,\theta)$ is below mean value than direction θ is degraded, and if Π_u is larger than A_u then θ receives a higher probability weight through q.

Putting the model for cell movement (5) together with the equation for the fibre network (10) we propose the following *transport model for mesenchymal motion in undirected tissues*

$$\begin{aligned} p_t + v \cdot \nabla p &= -\mu p + \mu \frac{q(t,x,\hat{v})}{\omega} \bar{p}, \\ q_t &= \kappa(\Pi_u(t,x,\theta) - A_u(t,x))\, \bar{p}(t,x) q(t,x,\theta), \end{aligned} \tag{12}$$

where Π_u is given by (8) and A_u is given by (11).

2.2.2 Directed tissue

Our assumptions for the tissue changes are very similar to the undirected case.

1. Again, the product $\theta \cdot \hat{v}$ gives information about the relative orientation of θ and $\hat{v}$. However, now we assume that most cutting occurs if the cell happens to move opposite to the fibre direction. There are two reasons for this assumption. First, moving against the grain of a fibre might be very costly, or even impossible without destroying the fibre. Secondly, if a cell is elongated along a fibre θ, then it will touch it in many locations. If the cell direction is opposite to θ, then protease can be produced at all those

contact sites. Similar to above we define a projection operator:

$$\Pi_d(t,x,\theta) = \frac{1}{\bar{p}(t,x)} \int_V \theta \cdot \hat{v}\, p(t,x,v) \mathrm{d}v, \tag{13}$$

which can be written as well as

$$\Pi_d(t,x,\theta) = \theta \cdot \bar{\hat{v}}, \quad \text{with} \quad \bar{\hat{v}} = \frac{1}{\bar{p}} \int_V \hat{v} p \mathrm{d}v,$$

and it satisfies

$$-1 \le \Pi_d \le 1.$$

2. As before we assume mass action kinetics $\bar{p}Q$, and
3. the constant $\kappa \ge 0$ describes the protease efficiency.

Then the equation for the fibre density reads

$$Q_t(t,x,\theta) = \kappa(\Pi_d(t,x,\theta) - 1)\, \bar{p}\, Q. \tag{14}$$

For the fibre distribution $q(t,x,\theta)$ we obtain:

$$q_t(t,x,\theta) = \kappa(\Pi_d(t,x,\theta) - A_d(t,x))\, \bar{p}(t,x) q(t,x,\theta), \tag{15}$$

with

$$A_d(t,x) = \int_{S^{n-1}} \Pi_d(t,x,\theta) q(t,x,\theta) \mathrm{d}\theta. \tag{16}$$

Together with the model for cell movement (5) we obtain a *transport model for mesenchymal motion in directed tissues*

$$\begin{aligned} p_t + v \cdot \nabla p &= -\mu p + \mu \frac{q(t,x,\hat{v})}{\omega} \bar{p}, \\ q_t &= \kappa(\Pi_d(t,x,\theta) - A_d(t,x))\, \bar{p}(t,x) q(t,x,\theta), \end{aligned} \tag{17}$$

where Π_d is given by (13) and A_d is given by (16).

In the next section we begin the analysis with a one-dimensional formulation of these models (12, 17). Although the fibre network are intrinsically three-dimensional it is very helpful to look at the one-dimensional versions. It will elucidate the set up of these models and it prepares the stage for the analysis of the general models in the following sections.

3 1-D models for mesenchymal motion

Also in the one-dimensional case we need to distinguish between directed and undirected tissues. Here we will treat the directed case first, since it is more general and the undirected case follows easily. We fix speed to $|v| = s$ and consider a one-dimensional domain. Then cells can only move to the right or left

$$p^+(t,x) = p(t,x,+s), \quad p^-(t,x) = p(t,x,-s),$$

respectively. The distribution $q(t,x,\theta)$ describes a bias of choosing right over left and vice versa. Here we use the notation

$$q^+(t,x) = q(t,x,+1), \quad q^-(t,x) = q(t,x,-1), \quad q^+(t,x) + q^-(t,x) = 1.$$

The two moments of q are given by

$$\mathbb{E}_q = q^+ - q^-, \quad \text{and} \quad \mathbb{V}_q = 1 - (q^+ - q^-)^2. \tag{18}$$

The one-dimensional transport equation (5) reads

$$\begin{aligned} p_t^+ + sp_x^+ &= -\mu p^+ + \mu q^+(p^+ + p^-), \\ p_t^- - sp_x^- &= -\mu p^- + \mu q^-(p^+ + p^-). \end{aligned} \tag{19}$$

3.1 Directed tissue

To find the equations for $q^\pm$ we look at the projection operator Π_d (13) and obtain

$$\Pi_d(t,x,\theta) = \frac{1}{p^+ + p^-}(\theta(+1)p^+ + \theta(-1)p^-),$$

which leads to the definitions of

$$\Pi_d^+ := \Pi_d(t,x,+1) = \frac{p^+ - p^-}{p^+ + p^-}, \quad \Pi_d^- := \Pi_d(t,x,-1) = \frac{p^- - p^+}{p^+ + p^-}.$$

We calculate the mean projection A_d as

$$A_d(t,x) = \Pi_d^+ q^+ + \Pi_d^- q^- = \frac{p^+ - p^-}{p^+ + p^-}(q^+ - q^-).$$

Then the equation for q^+ reads

$$\begin{aligned} q_t^+ &= \kappa(\Pi_d^+ - A_d)\bar{p}q^+ \\ &= \kappa\left(\frac{p^+ - p^-}{p^+ + p^-} - \frac{p^+ - p^-}{p^+ + p^-}(q^+ - q^-)\right)(p^+ + p^-)q^+ \\ &= \kappa(p^+ - p^-)(q^- - q^+ + 1)q^+, \end{aligned}$$

and a similar equation for q^-:

$$q_t^- = \kappa(p^+ - p^-)(q^- - q^+ - 1)q^-.$$

Together we have the following model for one-dimensional mesenchymal motion in directed tissue:

$$\begin{aligned} p_t^+ + sp_x^+ &= -\mu p^+ + \mu q^+(p^+ + p^-), \\ p_t^- - sp_x^- &= -\mu p^- + \mu q^-(p^+ + p^-), \\ q_t^+ &= \kappa(p^+ - p^-)(q^- - q^+ + 1)q^+, \\ q_t^- &= \kappa(p^+ - p^-)(q^- - q^+ - 1)q^-. \end{aligned} \tag{20}$$

It is easy to check that $q^+ + q^- = 1$ is an invariant to the second last equations. Moreover, $q^- - q^+ + 1 > 0$ and $q^- - q^+ - 1 < 0$. Hence for $p^+ > p^-$ the term $(p^+ - p^-)$ is positive and q^+ will increase while q^- decreases. Hence directionality is enhanced by system (20).

We now add and subtract the first two equations of (20) to obtain equations for the total population $\bar{p} = p^+ + p^-$ and the population flux $j = s(p^+ - p^-)$.

$$\begin{aligned} \bar{p}_t + j_x &= 0, \\ j_t + s^2\bar{p}_x &= -\mu j + \mu(q^+ - q^-)s\bar{p}. \end{aligned} \tag{21}$$

Similarly, we can transform equations three and four of (20) by building the sum and the difference. For the sum we get $(q^+ + q^-)_t = 0$, since the sum is constant 1. The difference is $\mathbb{E}_q$ and satisfies

$$\mathbb{E}_{qt} = \frac{\kappa}{s}j(1 - \mathbb{E}_q^2) = \frac{\kappa}{s}j\mathbb{V}_q. \tag{22}$$

Now we study three scalings which become relevant later for the n-dimensional model as well:

(1) The telegraph equation: To derive a second-order equation we differentiate (21) again

$$\begin{aligned} \bar{p}_{tt} + j_{xt} &= 0, \\ j_{xt} + s^2\bar{p}_{xx} &= -\mu j_x + s\mu((q^+ - q^-)\bar{p})_x. \end{aligned}$$

As we substitute j_{xt} from the second equation we find a damped wave equation with drift term:

$$\frac{1}{\mu}\,\bar{p}_{tt} + \bar{p}_t + \left(s\mathbb{E}_q\bar{p}\right)_x = \frac{s^2}{\mu}\,\bar{p}_{xx}, \tag{23}$$

where the drift velocity is given by the expectation of q (18). This in fact is characteristic to what follows for the n-dimensional case as well.

(2) The parabolic scaling: To derive a diffusion model we study the *parabolic scaling* of space and time. Let $\xi = \varepsilon x$ denote a macroscopic space scale and $\tau = \varepsilon^2 t$ denote a long time scale. As we rescale the telegraph equation (23) we obtain

$$\frac{\varepsilon^4}{\mu}\,\bar{p}_{\tau\tau} + \varepsilon^2\bar{p}_\tau + \varepsilon\left(s\mathbb{E}_q\bar{p}\right)_\xi = \varepsilon^2\,\frac{s^2}{\mu}\,\bar{p}_{\xi\xi}, \tag{24}$$

which means the dominating term is the drift term. To obtain terms of equal order of magnitude we assume that the expectation $\mathbb{E}_q$ is small:

$$\mathbb{E}_q(\tau,\xi) = \lim_{\varepsilon\to 0}\frac{1}{\varepsilon}\left(q^+\left(\frac{\tau}{\varepsilon^2},\frac{\xi}{\varepsilon}\right) - q^-\left(\frac{\tau}{\varepsilon^2},\frac{\xi}{\varepsilon}\right)\right) < \infty. \tag{25}$$

With this assumption we obtain from (24) to leading order a drift-diffusion model with diffusion constant $\frac{s^2}{\mu}$ and drift velocity $s\mathbb{E}_q$:

$$\bar{p}_\tau + \left(s\mathbb{E}_q(\tau,\xi)\bar{p}\right)_\xi = \frac{s^2}{\mu}\bar{p}_{\xi\xi}\ . \tag{26}$$

(3) The hydrodynamic scaling: Here we assume that $\sigma = \varepsilon t$, $\xi = \varepsilon x$. Then from (23) we find:

$$\frac{\varepsilon^2}{\mu}\,\bar{p}_{\sigma\sigma} + \varepsilon\bar{p}_\sigma + \varepsilon\left(s\mathbb{E}_q\bar{p}\right)_\xi = \frac{\varepsilon^2 s^2}{\mu}\,\bar{p}_{\xi\xi}$$

which, to leading order, gives a pure drift model

$$\bar{p}_\sigma + \left(s\mathbb{E}_q\bar{p}\right)_\xi = 0,$$

with drift velocity $s\mathbb{E}_q$ which is now of order 1 and not scaled by ε as in the previous case.

In this one-dimensional example we see already that the relative size of the drift velocity $s\mathbb{E}_q$ sets the stage for the appropriate macroscopic model. If $s\mathbb{E}_q$ is of order $O(1)$ relative to ε then the hydrodynamic scaling gives the leading order approximation. If $s\mathbb{E}_q$ is of order $O(\varepsilon)$ then the parabolic scaling applies.

For the n-dimensional model we will carry the analysis a bit further and we will show that, in the hydrodynamic scaling, the diffusion term appears as a first-order correction to the leading order drift term. The study of the one-dimensional example will be continued in Sect. 5.3.

3.2 Undirected tissue

For undirected tissue we get a projection term of

$$\Pi_u^{\pm} = \frac{1}{p^+ + p^-}(|\theta|p^+ + |\theta|p^-) = 1,$$

and a mean projection of $A_u = 1$. Hence

$$q_t^{\pm} = 0.$$

Then the one dimensional model for mesenchymal motion in an undirected tissue reads

$$\begin{aligned} p_t^+ + sp_x^+ &= -\mu p^+ + \mu q^+(p^+ + p^-), \\ p_t^- - sp_x^- &= -\mu p^- + \mu q^-(p^+ + p^-), \\ q_t^+ &= 0, \\ q_t^- &= 0. \end{aligned} \tag{27}$$

Since cells can only move parallel to the fibres there is no cutting at all. The transformation to a telegraph equation and the three scaling limits are identical to the case of directed tissue.

4 Mesenchymal motion in n-dimensions

In this section we study the three above mentioned scalings (1) moment closure (telegraph equation), (2) parabolic scaling, and (3) hyperbolic scaling for models (12) and (17). All these methods are well known and have been used in various contexts. For moment closure see for example Levermore [16] or Hillen [13], for parabolic scaling see Othmer and Hillen [14,19] or Chalub et al. [4] and Hwang et al. [15] for recent result; and a good exposition of the hydrodynamic scaling can be found in Dolak and Schmeiser [9]. We have several good reasons to consider all three methods applied to the transport equations for mesenchymal motion. First of all, these methods have not yet been applied to mesenchymal motion. In particular for the closure or scaling limit of the fibre equation (q-equation), details of these methods are needed. Secondly, we find an interesting relation between the macroscopic parameters of drift velocity and diffusion tensor to statistical properties of the fibre matrix, i.e. the mean fibre orientation and the variance-covariance matrix. The importance of these

terms can only be understood if the details of the approximations are given. Thirdly, typically these methods appear in different papers written by different authors. Here I like to compare the results and explain differences and similarities. A detailed comparison helps to judge which method to choose in a given situation. For example, a parabolic scaling in a drift dominated situation does not make sense.

As far as the analysis of the transport part of these models is concerned, we do not need to seperate the undirected and directed cases. However, as soon as we consider the q-equation we distinguish the two tissue classes.

4.1 Transport equations

In this section we study the transport equation for cell movement (5) where we assume for now that the tissue distribution $q(t,x,\theta)$ is given. During the calculations various new constants and variables will be used, primarily to keep the exposition as transparent as possible. We will define all necessary parameters right here, although their motivation might become clear only at a later stage. Given the directional distribution $q(t,x,\theta)$ we defined already the expectation $\mathbb{E}_q$ in (1), the variance $\mathbb{V}_q$ in (2), and the parameter ω in (4). Further we define an *effective drift velocity*

$$u := \frac{1}{\omega}\int_V v q(t,x,\hat{v})\mathrm{d}v, \tag{28}$$

and an *effective diffusion tensor*

$$D := \frac{1}{\omega}\int_V (v-u)(v-u)^T q(t,x,\hat{v})\mathrm{d}v. \tag{29}$$

These new quantities can be expressed in terms of the expectation and variance of q as follows:

$$u = \beta\mathbb{E}_q, \quad \text{with} \quad \beta = \begin{cases} \frac{s_2^{n+1}-s_1^{n+1}}{\omega(n+1)} & \text{for } V = [s_1,s_2]\times S^{n-1}, \\ s^n & \text{for } V = sS^{n-1}. \end{cases} \tag{30}$$

The diffusion tensor D can be simplified for the case of $V = sS^{n-1}$ to

$$D = s^2\mathbb{V}_q. \tag{31}$$

As mentioned earlier, in case of an undirected tissue we have always $u = \beta\mathbb{E}_q = 0$. Then the diffusion tensor D can also be related directly to the Variance of q,

by:

$$D = \alpha \mathbb{V}_q, \quad \text{with} \quad \alpha = \begin{cases} \frac{s_2^{n+2} - s_1^{n+2}}{\omega(n+2)} & \text{for } V = [s_1, s_2] \times S^{n-1}, \\ s^{n+1} & \text{for } V = sS^{n-1}. \end{cases} \tag{32}$$

4.1.1 Moment closure

In the derivation of the telegraph equation (23) for the 1-dimensional model we derived the corresponding moment system for $\bar{p}$ and j in (21). In that case the moment system was closed after the first moment. In n-dimensions, however, the moment system is never closed. We define the velocity moments of $p(t,x,v)$ as

$$\bar{p}(t,x) = \int_V p(t,x,v)\mathrm{d}v, \quad m^1(t,x) = \int_V v p(t,x,v)\mathrm{d}v,$$
$$m^2(t,x) = \int_V v v^T p(t,x,v)\mathrm{d}v.$$

Note that $\bar{p}$ is a scalar, m^1 a vector and m^2 a 2-tensor and using the earlier definitions we have $m^1 = \bar{v}\bar{p}$.

As we integrate Eq. (5) over V and use the fact that $\int_V q(t,x,\hat{v})\mathrm{d}v = \omega$ we find the conservation law

$$\bar{p}_t + \nabla m^1 = 0. \tag{33}$$

Now we multiply (5) by v and integrate to obtain

$$\begin{aligned} m^1_t + \nabla \cdot m^2 &= -\mu m^1 + \mu \bar{p} \int_V v \frac{q(t,x,\hat{v})}{\omega} \mathrm{d}v \\ &= -\mu m^1 + \mu \bar{p} \beta \mathbb{E}_q, \end{aligned} \tag{34}$$

where we used (30).

In Hillen [12] an L^2-minimization method has been introduced to close a corresponding moment system. The moment closure can be carried out for general cases (see Hillen [13]) but here we restrict ourselves to the case that the cells have a constant speed but can move in any direction, $V = sS^{n-1}$. Then the second moment $m^2(t,x)$ can be approximated as $m^2 \approx \frac{s^2}{n}\bar{p}$ (see [12]).

Using this moment closure we obtain from (33) and (34):

$$\begin{aligned} \bar{p}_t + \nabla m^1 &= 0, \\ m^1_t + \frac{s^2}{n} \nabla \bar{p} &= -\mu m^1 + \mu \bar{p}\, \beta \mathbb{E}_q. \end{aligned} \tag{35}$$

In the same spirit as in (23) we can derive a telegraph equation:

$$\frac{1}{\mu}\bar{p}_{tt} + \bar{p}_t + \nabla\big(\bar{p}\,\beta\mathbb{E}_q\big) = \frac{s^2}{n\mu}\,\Delta\bar{p}. \tag{36}$$

Again, the expectation of q gives a net drift $u = \beta\mathbb{E}_q$.

4.1.2 The parabolic scaling

We study the same parabolic time and space scaling as for the 1-dimensional case above:

$$\tau = \varepsilon^2 t, \quad \xi = \varepsilon x$$

for a small parameter $\varepsilon > 0$. Scaling of the transport equation (5) leads to

$$\varepsilon^2 p_\tau + \varepsilon v \cdot \nabla_\xi p = -\mu p + \frac{\mu}{\omega} q(\tau,\xi,\hat{v})\bar{p}. \tag{37}$$

We abbreviate the right-hand side of (37) and define for each (τ,ξ) a linear operator

$$\mathcal{L}\varphi := -\mu\varphi(v) + \frac{\mu}{\omega} q(\tau,\xi,\hat{v})\bar{\varphi}$$

for $\varphi \in L^2_q(V)$, where $L^2_q(V)$ denotes a weighted L^2-space with weight function $q^{-1}(\tau,\xi,\hat{v})$. Hence the weight, and also the space $L^2_q(V)$ depends on the chosen space-time point (τ,ξ).

For each (τ,ξ) we identify the kernel of $\mathcal{L}$:

$$\mathcal{L}\varphi = 0 \Longleftrightarrow -\mu\varphi(v) + \frac{\mu}{\omega} q(\tau,\xi,\hat{v})\bar{\varphi} = 0.$$

Thus

$$\varphi(v) = \frac{q(\tau,\xi,\hat{v})}{\omega}\bar{\varphi}.$$

The operator $\mathcal{L}$ is a compact Hilbert–Schmidt operator (see [14]) and for each (τ,ξ) we split $L^2_q(V)$ according to

$$L^2_q(V) = \langle q(\tau,\xi,\hat{v})\,\rangle + \langle q(\tau,\xi,\hat{v})\,\rangle^\perp,$$

where $\langle q\rangle$ denotes the subspace of $L^2_q(V)$ that is spanned by q. Then on $\langle q\rangle^\perp$ we can invert $\mathcal{L}$ (see also [14]):

$$\mathcal{F} := \big(\mathcal{L}|_{\langle q\rangle^\perp}\big)^{-1}.$$

To calculate the pseudo-inverse $\mathcal{F}$ we consider $\varphi(v) \in \langle q\rangle^\perp$ and solve

$$\mathcal{L}\psi = \varphi.$$

Since $\varphi(v) \in \langle q\rangle^\perp$ we have $\int_V \varphi(v) q(\tau,\xi,\hat{v}) \frac{dv}{q(\tau,\xi,\hat{v})} = \int_V \varphi(v) dv = 0$.

Now

$$\mathcal{L}\psi = \varphi \quad \Longleftrightarrow \quad -\mu\psi(v) + \frac{\mu}{\omega} q(\tau,\xi,\hat{v})\bar{\psi} = \varphi(v),$$

which gives

$$\psi(v) = -\frac{1}{\mu}\varphi(v) - \bar{\psi}\frac{q(\tau,\xi,\hat{v})}{\omega}.$$

For $\psi(v) \in \langle q\rangle^\perp$ we have also $\bar{\psi} = 0$, hence

$$\psi(v) = -\frac{1}{\mu}\varphi(v).$$

We summarize the above calculations in a Lemma:

Lemma 4.1 *For each (τ,ξ) we have $\mathcal{F} = \left(\mathcal{L}|_{\langle q\rangle^\perp}\right)^{-1} = -\frac{1}{\mu}$ as a multiplication operator.*

Now we come back to the scaled Eq. (37) and consider an expansion in ε

$$p(\tau,\xi,v) = p_0(\tau,\xi,v) + \varepsilon p_1(\tau,\xi,v) + \varepsilon^2 p_2(\tau,\xi,v) + \text{ h.o.t.}$$

where we assume that all mass is contained in the leading order term,

$$\int_V p_i(\tau,\xi,v)\mathrm{d}v = 0, \quad \text{for} \quad i \geq 1.$$

As we compare orders of ε we find to leading order

$\boldsymbol{\varepsilon^0}$**:** $0 = \mathcal{L}p_0$. Which implies $p_0(\tau,\xi,v) = \bar{p}(\tau,\xi)\frac{q(\tau,\xi,\hat{v})}{\omega}$.

The order ε-terms yield:

$\boldsymbol{\varepsilon^1}$**:**

$$(\nabla\cdot v)p_0 = \mathcal{L}p_1. \tag{38}$$

To solve this equation in $\langle q\rangle^\perp$ the left-hand side has to satisfy a solvability condition:

$$0 = \int_V (\nabla\cdot v)p_0 q(\tau,\xi,\hat{v})\,\frac{\mathrm{d}v}{q(\tau,\xi,\hat{v})} = \nabla\cdot\int_V \frac{vq(\tau,\xi,\hat{v})}{\omega}\mathrm{d}v\,\bar{p}(\tau,\xi) \tag{39}$$

which is satisfied if we assume

$$\mathbb{E}_q = \frac{1}{\beta\omega}\int_V v q(\tau,\xi,\hat{v})\mathrm{d}v = 0. \tag{40}$$

Then $p_1(\tau,\xi,v) = -\frac{1}{\mu\omega}(v\cdot\nabla)\big(\bar{p}(\tau,\xi)q(\tau,\xi,\hat{v})\big)$.

The second order terms are

ε^2:

$$p_{0\tau} + (v\cdot\nabla)p_1 = \mathcal{L}p_2.$$

The solvability condition reads $\int p_{0\tau} + \int v\cdot\nabla p_1 = 0$, which gives

$$\begin{aligned} 0 &= \frac{1}{\omega}\int_V \bar{p}_\tau(\tau,\xi)q(\tau,\xi,\hat{v})\mathrm{d}v + \nabla\cdot\int_V v\left(-\frac{1}{\mu\omega}(v\cdot\nabla)(\bar{p}\,q)\right)\mathrm{d}v \\ &= \bar{p}_\tau - \frac{1}{\mu\omega}\nabla\cdot\int_V v[(v\cdot\nabla\bar{p})q + (v\cdot\nabla q)\bar{p}]\mathrm{d}v \\ &= \bar{p}_\tau - \frac{1}{\mu\omega}\nabla\cdot\int_V vv^T q(\tau,\xi,\hat{v})\mathrm{d}v\cdot\nabla\bar{p} - \frac{1}{\mu\omega}\nabla\cdot\left(\int_V v(v\cdot\nabla q)\,\mathrm{d}v\bar{p}\right). \end{aligned}$$

Which gives the resulting parabolic limit equation:

$$\bar{p}_\tau = \frac{1}{\mu}\nabla\cdot\left(D(\tau,\xi)\nabla\bar{p} + \bar{p}\,\nabla D(\tau,\xi)\right), \tag{41}$$

with diffusion tensor given by (29).

Since for $\mathbb{E}_q = 0$ the diffusion tensor can be written as $\alpha\mathbb{V}_q$ (see (32)), the limit equation (41) can also be written as

$$\bar{p}_\tau = \frac{\alpha}{\mu}\nabla\,\nabla(\mathbb{V}_q(\tau,\xi)\bar{p}), \tag{42}$$

where $\nabla\,\nabla$ is not the Laplace operator Δ, since $\nabla\,\nabla$ acts on a 2-tensor $\mathbb{V}_q\bar{p}$. The product on the right-hand side is a scalar. Using tensor notation and summation over repeated indices the Eq. (42) can be written as

$$\bar{p}_\tau = \frac{\alpha}{\mu}\partial_i\partial_j\big(\mathbb{V}_q^{ij}(\xi)\bar{p}\big).$$

The diffusion term is given by the variance-covariance matrix of the underlying fibre network and since in (40) we assumed $\mathbb{E}_q = 0$ there is no drift term in (42).

In the case of chemotaxis transport equations the convergence of solutions for $\varepsilon \to 0$ has been rigorously shown in Chalub et al. [4] and Hwang et al. [15].

As mentioned earlier, these theories do not apply here, since we need to include fibre networks distributions q in the class of distributions.

4.1.3 The hydrodynamic scaling

In the previous section we assumed that the transport is diffusion dominated and directed drift does not play an important role ($\mathbb{E}_q = 0$ in (40)). The framework of hydrodynamic scaling is applicable even if $\mathbb{E}_q = \mathcal{O}(1)$ and it can be clearly seen that the assumption $\mathbb{E}_q = O(\varepsilon)$ is necessary to obtain a pure diffusion limit. In this section we first derive a drift approximation and in a second step a diffusion correction to the drift approximation.

As in Sect. 2.3 we study a hydrodynamic space and time scaling of

$$\sigma = \varepsilon t, \quad \xi = \varepsilon x.$$

Then the transport equation (5) becomes

$$\varepsilon p_\sigma + \varepsilon(v \cdot \nabla)p = \mathcal{L}p. \tag{43}$$

Again, we use the operator properties of $\mathcal{L}$ and split the solution into two parts:

$$p(\sigma, \xi, v) := \bar{p}(\sigma, \xi)\frac{q(\sigma, \xi, \hat{v})}{\omega} + \varepsilon p^\perp(\sigma, \xi, v) \tag{44}$$

$$\text{with} \quad \int_V p^\perp(\sigma, \xi, v)\mathrm{d}v = 0.$$

This approximation technique is also known as the *Chapman–Enskog expansion* in physical context. We closely follow the exposition as used by Dolak and Schmeiser [9] for chemotaxis. The results of [9] do not apply to our system directly, but the essential steps are very similar.

We substitute (44) into (43) and obtain:

$$\begin{aligned}\varepsilon\bar{p}_\sigma\frac{q}{\omega} + \varepsilon\bar{p}\frac{q_\sigma}{\omega} + \varepsilon^2 p^\perp_\sigma + \varepsilon(v \cdot \nabla)(\bar{p}\frac{q}{\omega}) + \varepsilon^2(v \cdot \nabla)p^\perp &= \mathcal{L}\left(\bar{p}\frac{q}{\omega} + \varepsilon p^\perp\right) \\ &= \varepsilon\mathcal{L}p^\perp. \end{aligned} \tag{45}$$

As we integrate (45) over V and divide by ε we get

$$\bar{p}_\sigma + \nabla \cdot \left(\frac{1}{\omega}\int_W vq\, dv\, \bar{p} + \varepsilon \int vp^\perp dv\right) = 0, \tag{46}$$

where we used the fact that

$$\int_V q_\sigma \mathrm{d}v = \frac{\partial}{\partial\sigma}\int_V q\mathrm{d}v = 0, \quad \text{and} \quad \int_V p^\perp_\sigma \mathrm{d}v = \frac{\partial}{\partial\sigma}\int_W p^\perp \mathrm{d}v = 0.$$

Again, the mean value of q over V appears

$$\bar{p}_\sigma + \nabla\cdot\left(\beta\,\mathbb{E}_q\bar{p} + \varepsilon\int_V v p^\perp \mathrm{d}v\right) = 0. \tag{47}$$

To leading order this is a drift-dominated model

$$\bar{p}_\sigma + \nabla\cdot(\beta\,\mathbb{E}_q\bar{p}) = 0. \tag{48}$$

In the next step we need to find an expression for $p^\perp$. To keep the following calculations transparent we will use the effective drift u and the effective diffusion tensor D as defined in (30) and (31). From (47) we can obtain $\bar{p}_\sigma$ and substitute this into (45) (and divide by ε):

$$\begin{aligned}\mathcal{L}p^\perp &= -\frac{q}{\omega}\nabla\cdot\left(u\bar{p} + \varepsilon\int_V v p^\perp \mathrm{d}v\right) + \bar{p}\frac{q_\sigma}{\omega} + \varepsilon p^\perp_\sigma + \frac{1}{\omega}(v\cdot\nabla)(\bar{p}q) + \varepsilon(v\cdot\nabla)p^\perp \\ &= \frac{1}{\omega}(v\cdot\nabla)(\bar{p}q) - \frac{q}{\omega}\nabla\cdot(u\bar{p}) + \frac{1}{\omega}\bar{p}q_\sigma + O(\varepsilon).\end{aligned} \tag{49}$$

To leading order we obtain, after rearrangement:

$$\mathcal{L}p^\perp \approx \frac{q}{\omega}(v-u)\cdot\nabla\bar{p} + \frac{1}{\omega}(v\cdot\nabla q - q\nabla\cdot u + q_\sigma)\bar{p}. \tag{50}$$

We apply the pseudo inverse of $\mathcal{L}$ and find

$$p^\perp \approx -\frac{1}{\mu\omega}\left(q(v-u)\cdot\nabla\bar{p} + (v\cdot\nabla q - q\nabla\cdot u + q_\sigma)\bar{p}\right). \tag{51}$$

We substitute $p^\perp$ into (47) and we switch to tensor notation where we use the summation convention for repeated indices. This avoids confusion about multiple products of vectors and their derivatives. As we use (51) in (47) we

obtain

$$\begin{aligned}
&\bar{p}_\sigma + \partial_j(u_j\bar{p}) \\
&\quad = \frac{\varepsilon}{\mu\omega}\partial_j\left(\int_V v_j\Big[q(v_i-u_i)\partial_i\bar{p} + (v_i\partial_i q - q\partial_i u_i + q_\sigma)\bar{p}\Big]\mathrm{d}v\right) \\
&\quad = \frac{\varepsilon}{\mu\omega}\partial_j \int_V v_j(v_i-u_i)q\,\mathrm{d}v\,\partial_i\bar{p} \\
&\qquad + \frac{\varepsilon}{\mu\omega}\partial_j\left(\left[\int_V v_j(v_i\partial_i q - q\frac{1}{\omega}\int_V v_i'\partial_i q\,\mathrm{d}v')\mathrm{d}v + \omega u_{j\sigma}\right]\bar{p}\right).
\end{aligned}$$

The two integrals inside the square brackets can be written as

$$\begin{aligned}
&\int_V v_j(v_i\partial_i q - q\frac{1}{\omega}\int_V v_i'\partial_i q\,\mathrm{d}v')\mathrm{d}v \\
&\quad = \int_V v_j v_i\partial_i q\,\mathrm{d}v - \frac{1}{\omega}\int_V v_j q\,\mathrm{d}v\int_V v_i'\partial_i q\,\mathrm{d}v' \\
&\quad = \int_V (v_j-u_j)v_i\partial_i q\,\mathrm{d}v \\
&\quad = \int_V (v-u)\,v^T\cdot\nabla q\,\mathrm{d}v,
\end{aligned}$$

where we returned to vector notation in the last step. Hence we obtain

$$\begin{aligned}
\bar{p}_\sigma + \nabla\cdot(u\bar{p}) = \frac{\varepsilon}{\mu\omega}\nabla\cdot\int_V v(v-u)^T q\,\mathrm{d}v\cdot\nabla\bar{p} \\
+\frac{\varepsilon}{\mu\omega}\nabla\cdot\left(\left(\int_V (v-u)(v^T\cdot\nabla q)\mathrm{d}v + \omega u_\sigma\right)\bar{p}\right). \qquad (52)
\end{aligned}$$

We use the diffusion tensor (29) to write the term on the right-hand side in a more compact form. Note that we always have

$$\frac{1}{\omega}\int_V v(v-u)^T q(\sigma,\xi,\hat{v})\mathrm{d}v = \frac{1}{\omega}\int_V (v-u)(v-u)^T q(\sigma,\xi,\hat{v})\mathrm{d}v = D,$$

As we study $\nabla D(\sigma,\xi)$ we find:

$$\begin{aligned}\partial_i D(\sigma,\xi) &= \frac{1}{\omega}\int_V v_i\partial_i(v_j-u_j)q + v_i(v_j-u_j)\partial_i q \,\mathrm{d}v\\ &= -\frac{1}{\omega}\int_V v_i q\,\mathrm{d}v\partial_i u_j + \frac{1}{\omega}\int_V v_i(v_j-u_j)\partial_i q\,\mathrm{d}v\\ &= u_i\partial_i u_j + \frac{1}{\omega}\int_V v_i(v_j-u_j)\partial_i q\,\mathrm{d}v.\end{aligned}$$

Then with (52) we arrive at the equation

$$\bar{p}_\sigma + \nabla\cdot(u\bar{p}) = \frac{\varepsilon}{\mu}\nabla\big(\nabla(D(\sigma,\xi)\bar{p}) + [u(\nabla\cdot u) + u_\sigma]\bar{p}\big) \tag{53}$$

with a time-dependent drift term

$$u(\sigma,\xi) = \frac{1}{\omega}\int_V vq(\sigma,\xi,\hat{v})\,\mathrm{d}v = \beta\mathbb{E}_q \tag{54}$$

and a time-dependent diffusion tensor

$$D(\sigma,\xi) = \frac{1}{\omega}\int_V v(v-u(\sigma,\xi))^T q(\sigma,\xi,\hat{v})\mathrm{d}v. \tag{55}$$

Note that if $u\approx 0$ we obtain the same diffusion terms as from the parabolic scaling in (41). Note also that D is positive definite and symmetric since it can be written as

$$D = \frac{1}{\omega}\int_V (v-u(\sigma,\xi))(v-u(\sigma,\xi))^T q(\sigma,\xi,\hat{v})\mathrm{d}v.$$

4.2 Examples

Example 1 (Unidirectional tissue)

As an example we consider a strictly aligned tissue. We choose the coordinate axis e_1 in the direction of the tissue alignment and we assume

$$q(\sigma,\xi,\theta) = \begin{cases} 0.5 & \text{if } \theta = e_1,\\ 0.5 & \text{if } \theta = -e_1,\\ 0 & \text{otherwise.}\end{cases}$$

Further we assume that the cells have a preferred speed s, hence $V = sS^{n-1}$. In that case we find

$$\omega = s^{n-1}, \quad u = 0, \quad D = s^2 e_1 e_1^T.$$

Then the limit equation (53) becomes a one-dimensional diffusion equation in direction of the tissue alignment:

$$\bar{p}_\sigma = \frac{\varepsilon s^2}{\mu} \bar{p}_{\xi_1,\xi_1}.$$

Example 2 (Spatially homogeneous)
If the tissue is timely constant and spatially homogeneous, i.e. $q(\sigma,\xi,\theta) = q(\theta)$, then we obtain

$$\bar{p}_\sigma + \nabla \cdot (u\bar{p}) = \frac{\varepsilon}{\mu} \nabla \cdot D\nabla \bar{p},$$

where u is a constant vector and D is a constant matrix.

Example 3 (Fixed speed)
The case of fixed cell speed $V = sS^{n-1}$ is very interesting and it is worthwhile to summarize the result for this case. We find

$$\omega = s^{n-1}, \quad u(\sigma,\xi) = s\mathbb{E}_q, \quad D(\sigma,\xi) = s^2 \mathbb{V}_q.$$

The resulting macroscopic model now reads

$$\bar{p}_\sigma + s\nabla \cdot \left(\mathbb{E}_q \bar{p}\right) = \frac{\varepsilon s^2}{\mu} \nabla \Big(\nabla(\mathbb{V}_q\, \bar{p}) + \mathbb{E}_q (\nabla \cdot \mathbb{E}_q)\bar{p} + \frac{1}{s} \mathbb{E}_{q,\sigma} \bar{p} \Big), \tag{56}$$

where the statistical properties of the tissue enter the equations directly via the expectation $\mathbb{E}_q$ and the variance-covariance matrix $\mathbb{V}_q$.

Example 4 (Relation to vector fields and ODE's)
There is a natural relation of the mesenchymal motion models to ordinary differential equations (ODEs). A solution of an ODE

$$\dot{x} = f(t,x) \tag{57}$$

can be understood as an orbit $x(t)$ that follows the vector field $f(t,x)$ such that at each point the vector f is tangential to the orbit. To connect this ODE to our model we assume that $\|f\| = 1$. In the language of our modeling, a given vector field $f(t,x)$ corresponds to a given, well defined orientational vector for each (σ,ξ), hence

$$q(\sigma,\xi,\theta) = \delta_{f(\sigma,\xi)}(\theta).$$

Hence the vector field f becomes a directed fibre network q. The corresponding macroscopic quantities can be easily computed. The drift velocity is

$$u = \beta f(\sigma, \xi)$$

where the constant parameter β was given in (30). The diffusion matrix D for this case is zero, which makes sense, since the variance of the fibre distribution is zero for a uniquely defined orientation vector. Hence the macroscopic limit is purely drift dominated and becomes

$$\bar{p}_\sigma + \nabla(\beta f(\sigma, \xi)\bar{p}) = 0.$$

This is a hyperbolic differential equation and the characteristics are given by

$$\dot{x} = \beta f(t, x),$$

which corresponds to a scaled version of the ODE (57). Hence in a given vector field f the cells move along orbits of the ODE. The same argument can be made, if we relax the assumption that $\|f\| = 1$. In that case only the constant β would change. The interpretation in the context of cells moving along the orbit of an ODE remains the same. In this sense, the model for mesenchymal motion generalizes ODE's to a situation that the vector field is only given by a probability distribution function q.

5 Macroscopic models with protease dynamics

Now we use the above observations to study the protease-tissue interaction models (10) for undirected tissue and (15) for directed tissue.

5.1 Undirected tissue

The equation for protease interaction with an undirected tissue is given by (10), with projection operator (8) and mean projection length (11). The projection operator Π_u uses the integration over the particle distribution function $p(\sigma, \xi, v)$. To obtain an equation that only depends on $\bar{p}$ and q we use the Chapman–Enskog expansion again $p = \bar{p}\frac{q}{\omega} + \varepsilon p^\perp$. Then to leading order we find

$$\Pi_u(\sigma, \xi, \theta) \approx \int_V |\theta \cdot \hat{v}| \frac{q(\sigma, \xi, \hat{v})}{\omega} \mathrm{d}v = \int_{S^{n-1}} |\theta \cdot \theta'| q(\sigma, \xi, \theta') \mathrm{d}\theta', \tag{58}$$

and

$$A_u(\sigma, \xi) = \int_{S^{n-1}} \Pi_u(\sigma, \xi, \theta) q(\sigma, \xi, \theta) \mathrm{d}\theta. \tag{59}$$

Since, as mentioned earlier, for an undirected tissue we have $u = \beta \mathbb{E}_q = 0$, we arrive at the following full *macroscopic model for mesenchymal motion in undirected tissue*

$$\bar{p}_\sigma = \frac{1}{\mu}\nabla\Big[\nabla(D\bar{p})\Big], \tag{60}$$

$$\varepsilon q_\sigma = \kappa(\Pi_u - A_u)\bar{p}q, \tag{61}$$

$$D(\sigma,\xi) = \alpha \mathbb{V}_q(\sigma,\xi), \tag{62}$$

$$\Pi_u(\sigma,\xi,\theta) = \int\limits_{S^{n-1}} |\theta\cdot\theta'| q(\sigma,\xi,\theta')\mathrm{d}\theta', \tag{63}$$

$$A_u(\sigma,\xi) = \int\limits_{S^{n-1}} \Pi_u(\sigma,\xi,\theta) q(\sigma,\xi,\theta)\mathrm{d}\theta. \tag{64}$$

System (60)–(64) forms a closed system for the total cell density $\bar{p}(\sigma,\xi)$ and the fibre network $q(\sigma,\xi,\theta)$. In the undirected case, the drift diffusion approximation becomes a pure diffusion model (60), where the anisotropic diffusion tensor D, given by (62), is proportional to the variance-covariance matrix of the underlying fibre network. The fibre degradation dynamics in Eq. (61) are now almost entirely described by the fibre directional distribution $q(\sigma,\xi,\theta)$. The dependence on the cell population occurs only via multiplication with $\bar{p}$.

5.2 Directed tissue

In case of a directed tissue the equation for protease interaction with the tissue is given by (15), with projection operator (13) and mean projection length (16). As we use the Chapman–Enskog expansion $p = \bar{p}\frac{q}{\omega} + \varepsilon p^\perp$ for Π_d we obtain to leading order

$$\Pi_d(\sigma,\xi,\theta) \approx \theta\cdot\mathbb{E}_q, \tag{65}$$

and

$$A_d(\sigma,\xi) = \mathbb{E}_q^2. \tag{66}$$

Together with the drift-diffusion model derived earlier (53) we arrive at the following *macroscopic model for mesenchymal motion in directed tissue*

$$\bar{p}_\sigma + \nabla\cdot(u\bar{p}) = \frac{\varepsilon}{\mu}\nabla\big(\nabla(D(\sigma,\xi)\bar{p}) + [u(\nabla\cdot u) + u_\sigma]\bar{p}\big), \tag{67}$$

$$\varepsilon q_\sigma = \kappa(\theta\cdot\mathbb{E}_q - \mathbb{E}_q^2)\bar{p}q, \tag{68}$$

$$u(\sigma,\xi) = \beta\mathbb{E}_q, \tag{69}$$

$$D(\sigma,\xi) = \frac{1}{\omega}\int\limits_V (v-u)(v-u)^T q(\sigma,\xi,\hat{v})\mathrm{d}v. \tag{70}$$

In addition to a non-isotropic diffusion term D in (67) the expectation of q is an important ingredient. We obtain a dominating drift term with drift velocity u and a drift-diffusion correction term $u(\nabla \cdot u) + u_\sigma$. This term is a directional derivative of u in the mean movement direction. A term of this form is known from the Navier–Stokes equation modeling fluid flow [20]. The projection and fibre degradation are now given through the drift velocity term $\mathbb{E}_q$. The cell population appears as a multiplicator in (68) only.

5.3 The one-dimensional case revisited

In Sect. 3 we studied one-dimensional versions of the mesenchymal motion models for directed and undirected fibre networks. If we apply the limit equations for undirected tissue (60)–(64) to the one-dimensional case directly, we obtain

$$\Pi_u = 1, \quad A_u = 1, \quad q_\sigma^\pm = 0, \quad D = \alpha \mathbb{V}_q = s^2,$$

and we obtain the one-dimensional diffusion model

$$\bar{p}_\sigma = \frac{s^2}{\mu} \bar{p}_{\xi\xi}. \tag{71}$$

This model coincides with the drift diffusion model (26) for $\mathbb{E}_q = 0$, which was derived by direct methods in Sect. 3.

For the directed case we find from (67)–(70)

$$\bar{p}_\sigma + s(\mathbb{E}_q \bar{p})_\xi = \frac{\varepsilon s^2}{\mu} \left(((1 - \mathbb{E}_q^2)\bar{p})_\xi + \left[\mathbb{E}_q \mathbb{E}_{q,\xi} + \frac{1}{s} \mathbb{E}_{q,\sigma} \right] \bar{p} \right)_\xi, \tag{72}$$

$$\varepsilon q_\sigma^\pm = \kappa (q^+ - q^-) \bar{p} (q^- - q^+ \pm 1) q^\pm, \tag{73}$$

$$\mathbb{E}_q = q^+ - q^-. \tag{74}$$

In this case the expectation of q also enters the diffusion term through $1 - \mathbb{E}_q^2$. In Sect. 3 we derived a one-dimensional model for mesenchymal motion in a directed tissue as system (20). If we compare the last two equations of (20) with equation (73) we see that the difference $p^+ - p^-$ in (20) has been replaced by the term $\bar{p}(q^+ - q^-)$ in (73). Hence in (73) the difference in right or left moving cells is approximated by the difference in fibre orientation multiplied by the total number of cells.

6 Discussion

In this paper we used kinetic transport equations to model mesenchymal motion of cells in fibre networks. It turns out that a distinction between directed and undirected tissues is important. The mesoscopic models (12) and (17) consist

of a transport equation for the cell movement coupled to a system of ordinary differential equations for the tissue fibres. It is assumed that the tissue fibre distribution gives the most probable movement direction of the cells. It is remarkable that the drift-diffusion limits (60)–(64) and (67)–(70) are almost entirely based on two statistical quantities of the fibre network, the expectation $\mathbb{E}_q$ as net drift and the variance-covariance matrix $\mathbb{V}_q$ as effctive diffusion matrix.

In this paper, two very specific cell-fibre inteactions have been modelled, using effective projection operators Π_u and Π_d to describe proteolytic fibre degradation. I abstained from the possibility to formulate a most general scaling result. For that the general fibre network equation $q_t = G(\theta, p, q)$ needs to be studied. Using the Chapman–Enskog expansion $p = \bar{p}\frac{q}{\omega} + \varepsilon p^{\perp}$ in G we are let to

$$G(\theta, p, q) = G\left(\theta, \bar{p}\frac{q}{\omega}, q\right) + \varepsilon p^{\perp}\frac{\partial G}{\partial p} + \mathcal{O}(\varepsilon^2),$$

and the fibre network equation for the macroscopic limit reads

$$q_t = G\left(\theta, \bar{p}\frac{q}{\omega}, q\right).$$

A general function G can include fibre production through fibroblasts for example. A connection to the wound healing model of Dallon and Sherratt [5] needs to be investigated in more detail in future work.

The discussion of the one-dimensional versions is not significant for applications, since movement in fibre networks is a three-dimensional process. However, the corresponding one-dimensional models (20) and (27) are very instructive and they provide some basic insight into the mechanisms involved. For example, the existence of traveling pulse solutions for the one-dimensional case is studied in Wang et al. [23].

The macroscopic models derived in (60)–(64) and in (67)–(70) use non-isotropic diffusion. Through recent developments in MRI spectroscopy the non-isotropic diffusion tensors can be measured by the DTI method [3]. With DTI imaging we might be able to parametrize directed tissue. Then, with our model, we could study the movement and spread of cancerous cells in these directed tissues. It would be worthwhile for future research to attempt to model cell movement in the white matter tracks in the brain of animals (see Mori's work [17]).

Mathematically the drift-diffusion limits are very interesting and results for chemotaxis applications can be found in Chalub et al. [4] and Hwang et al. [15]. These methods do not apply here, since delta-distributions for the fibre network q need to be included in an existence theory. We illustrated a natural relation to ODEs for the case that at each location there is a given unique orientational vector. A detailed mathematical analysis of these models is quite involved and goes beyond the scope of this paper. We are currently working on stability analysis, numerical schemes, and appropriate and realistic boundary conditions.

Dickinson [8] derived a macroscopic drift-diffusion model for contact guidance using projection methods applied to a Fokker–Planck equation. The Fokker–Planck equation describes the time evolution of the joint probability distribution of the cell location r and the cell orientation θ. The cell orientation was assumed to change continuously in time which was expressed through rotational drift and rotational diffusion terms. In Dickinson [7] the model was generalized to include discrete orientational changes that are triggered by a Poisson process (see also velocity jump process [18]). Our model from Sect. 4 for the case of a timely constant tissue is a special case of Dickinson's model, although the methods used are different. Here we will apply Dickinson's results to the model (5) for the case of timely constant tissue $q(x,\theta)$ and relate the relevant parameters explicitly. The drift-diffusion limit in [7] has the form

$$p_t(x,t) = -\nabla(V(x)p(x,t)) + \nabla^T(M(x)\nabla p(x,t)) \tag{75}$$

with *random motility tensor*

$$M(x) = \frac{1}{\mu\omega}\int_W (v-u)v^T q(x,\hat{v})\mathrm{d}v = \mu D(x)$$

and drift velocity

$$V(x) = u + \frac{1}{\mu\omega}\int_W (v-u)v^T \nabla q(x,\hat{v})\mathrm{d}v.$$

Using some vector calculus it can be shown that equation (75) is identical to model (67) for timely constant $q(x,\theta)$. Other relevant relations are as follows, where the left-hand side of the equations refers to Dickinson's notation and the right-hand side corresponding to the notation used in this paper:

$$\eta^{-1} = \varepsilon, \quad \bar{v}(r) = u, \quad L^{-1}(1-P) = -\mu^{-1}$$
$$\Delta = -\varepsilon\mu^{-1}(v-u), \quad \Gamma = v\omega^{-1}q(x,\hat{v}), \quad p_s(\sigma_0,r) = \omega^{-1}q(x,\hat{v}).$$

In [7] time-varying tissues are also considered. It is, however, assumed that the changes occur on a different timescale than cell movement such that the equilibrium distribution $p_s(\sigma_0,r)$ is quasi-stationary. This condition is not needed here and we consider the case where $q(t,x,\hat{v})$ changes dynamically over time. This leads to a coupled dynamical system between the cell movement and the tissue changes.

The *anisotropic biphasic theory* (ABT) of Barocas and Tranquillo [2] is based on mass and momentum balance equations between the tissue-cell phase and the interstitial fluid phase. The fibre orientations are described by a matrix $\Omega_f = \mathbb{V}_q$ (in our notation). It is assumed that the cell alignment, expressed

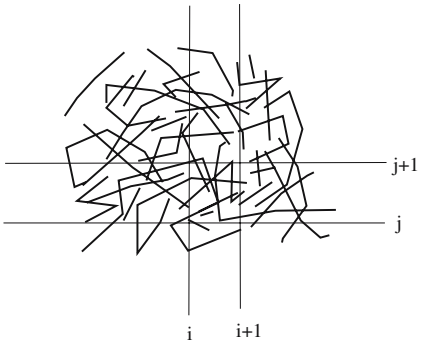

Fig. 3 An example of a two-dimensional tissue

through a matrix Ω_c, follows the fibre alignment as

$$\Omega_c = \frac{3}{\text{trace}(\Omega_f)^k}(\Omega_f)^k,$$

for some $k > 0$. In this sense, the orientation is instantaneous and not dynamical as in our model. Examples of how to calculate Ω_f, Ω_c in specific two-or three-dimensional situations and possible applications to wound healing are given in Barocas and Tranquillo [2,22].

To apply the above model for mesenchymal motion one needs an efficient numerical solver and one needs to identify appropriate initial conditions for $\mathbb{E}_q$ and $\mathbb{V}_q$. Initial conditions for the population density $\bar{p}(0,x)$ can be easily formulated according to an experimental setup. To get an initial condition for q the following procedure can be used. In two dimensions any direction in S^1 can be characterized by one angle $\alpha \in [-\pi,\pi]$ and $\theta = (\cos(\alpha), \sin(\alpha))$. In three space dimensions two angles would be needed $\theta = (\cos(\alpha)\sin(\beta), \sin(\alpha)\sin(\beta), \cos(\beta))$.

Now assume that a two-dimensional tissue of undirected fibres is given as in Fig. 3. The two-dimensional area will be divided into cells $C(i,j)$ and the angle of all tissue fibres inside $C(i,j)$ will be measured. For the cell shown in Fig. 1 we find the angles (in degree): $\alpha_j = 110, 110, 150, 20, 25, 100, 10, 95, 110, 90, 40, 45, 175$, where we only use angles between 0 and 180°. We assume that the fibres are undirected and we add the values of $180 + \alpha_j$. Hence for the cell $C(i,j)$ we find the angle distribution of $\alpha_j = 110, 110, 150, 20, 25, 100, 10, 95, 110, 90, 40, 45, 175, 290, 290, 330, 200, 205, 280, 190, 175, 290, 270, 220, 225, 355$, and each of these angles can be chosen with probability $q(\theta(\alpha_j)) = 1/26$. Then q is defined and the mean direction and the variance-covariance matrix can be calculated as

$$\mathbb{E}_q = \begin{pmatrix} -0.04 \\ 0.04 \end{pmatrix}, \quad \mathbb{V}_q = \begin{pmatrix} 0.49 & 0 \\ 0 & 0.51 \end{pmatrix}.$$

Here we see that the fibre network is, in the mean, oriented in the direction $(-1, 1)$ and the diffusion constants in x and y direction differ only slightly.

Overall the mesoscopic and macroscopic models derived here form a fruitful framework for modeling of advection and diffusion in a highly non-homogeneous oriented environments. The models are very promising for applications to tumor metastasis in directed tissue, for wound healing, and also for network formation. Of course, the use of these models needs to be tested against experiments.

Acknowledgements I am grateful for helpful remarks and discussions with K.P. Hadeler, and K. Painter. Thanks also to B. Hatzikirou, who told me about the DTI method. The comments of anonymous referees were a great help to improve this manuscript. This work was supported by NSERC.

References

1. Alt, W.: Singular perturbation of differential integral equations describing biased random walks. J. Reine Angew. Math. **322**, 15–41 (1981)
2. Barocas, V.H., Tranquillo, R.T.: An anisotropic biphasic theory of tissue-equivalent mechanics: The interplay among cell traction, fibrillar network deformation, fibril alignment and cell contact guidance. J. Biomech. Eng. **119**, 137–145 (1997)
3. Berenschot, G.: Vizualization of Diffusion Tensor Imaging. Eindhoven University of Technology, Master Thesis (2003)
4. Chalub, F.A.C.C., Markovich, P.A., Perthame, B., Schmeiser, C.: Kinetic models for chemotaxis and their drift-diffusion limits. Monatsh. Math. 123–141 (2004)
5. Dallon, J.C., Sherratt J.A.: A mathematical model for spatially varying extracellular matrix alignment. SIAM J. Appl. Math. **61**, 506–527 (2000)
6. Dallon, J.C., Sherratt, J.A., Maini, P.K.: Modelling the effects of transforming growth factor-β on extracellular alignment in dermal wound repair. Wound Rep. Reg. **9**, 278–286 (2001)
7. Dickinson, R.: A generalized transport model for biased cell migration in an anisotropic environment. J. Math. Biol. **40**, 97–135 (2000)
8. Dickinson, R.B.: A model for cell migration by contact guidance. In: Alt, W., Deutsch, A., Dunn, G. (eds) Dynamics of Cell and Tissue Motion, pp. 149–158, Birkhauser, Basel, (1997)
9. Dolak, Y., Schmeiser, C.: Kinetic models for chemotaxis: Hydrodynamic limits and spatio-temporal mechanics. J. Math. Biol. **51**, 595–615 (2005)
10. Friedl, P., Bröcker, E.B.: The biology of cell locomotion within three dimensional extracellular matrix. Cell Motility Life Sci. **57**, 41–64 (2000)
11. Friedl, P., Wolf, K.: Tumour-cell invasion and migration: diversity and escape mechanisms. Nat. Rev. **3**, 362–374 (2003)
12. Hillen, T.: On L^2-closure of transport equations: the Cattaneo closure. Discrete Cont. Dyn. Syst. B **4**(4), 961–982 (2004)
13. Hillen, T.: On the L^2-closure of transport equations: the general case. Discrete Cont. Dyn. Syst. B **5**(2), 299–318 (2005)
14. Hillen, T., Othmer, H.G.: The diffusion limit of transport equations derived from velocity jump processes. SIAM J. Appl. Math. **61**(3), 751–775 (2000)
15. Hwang, H.J., Kang, K., Stevens, A.: Global solutions of nonlinear transport equations for chemosensitive movement. SIAM J. Math. Anal. **36**, 1177–1199 (2005)
16. Levermore, C.D.: Moment closure hierarchies for kinetic theories. J. Stat. Phys. **83**, 1021–1065 (1996)
17. Mori, S., Crain, B.J., Chacko, V.P., Zijl, P.C.M.: Three-dimensional tracking of axonal projections in the brain by magnetic resonance imaging. Ann. Neurol. **45**, 265–269 (1999)
18. Othmer, H.G., Dunbar, S.R., Alt, W.: Models of dispersal in biological systems. J. Math. Biol. **26**, 263–298 (1988)
19. Othmer, H.G., Hillen, T.: The diffusion limit of transport equations II: Chemotaxis equations. SIAM J. Appl. Math. **62**(4), 1122–1250 (2001)

20. Robinson, J.C.: Infinite-Dimensional Dynamical Systems. Cambridge Texts in Applied Mathematics. Cambridge University Press, Cambridge (2001)
21. Stevens, A.: The derivation of chemotaxis-equations as limit dynamics of moderately interacting stochastic many particle systems. SIAM J. Appl. Math. **61**(1), 183–212 (2000)
22. Tranquillo, R.T., Barocas, V.H.: A continuum model for the role of fibroblast contact guidance in wound contraction. In: Alt, W., Deutsch, A., Dunn, G. (eds) Dynamics of Cell and Tissue Motion, pp. 159–164, Birkhauser, Basel (1997)
23. Wang, Z., Hillen, T., Li, M.: Global existence and travling waves to models for mesenchymal motion in one dimension. (in preparation) 2006
24. Wolf, K., Mazo, I., Leung, H., Engelke, K., von Andria, U., Deryngina, E. I., Strongin, A.Y., Bröcker, E.B., Friedl, P.: Compensation mechanism in tumor cell migration: mesenchymal-amoeboid transition after blocking of pericellular proteolysis. J. Cell Biol. **160**, 267–277 (2003)
25. Yurchenco, P.D., Birk, D.E., Mechan, R. P.: Extracellular Matrix Assembly. Academic Press, San Diego (1994)